PAPER

Cite this: *RSC Adv.*, 2018, **8**, 28024

Effect of SiO2 amount on heterogeneous base catalysis of SiO2@Mg–Al layered double hydroxide†

Mahiro Shirotori,[a] Shun Nishimura [ID] *[ab] and Kohki Ebitani*[ab]

The effects of SiO_2 amount on the base catalysis of highly active finely crystallized Mg–Al type layered double hydroxides prepared by the co-precipitation method with coexistence of SiO_2 spheres, denoted as SiO_2@LDHs, were investigated. With the Si/(Mg + Al) atomic ratios of 0–0.50, the highest activity for the Knoevenagel condensation was observed in the case of Si/(Mg + Al) = 0.17, as the reaction rate of 171.1 mmol g(cat)$^{-1}$ h^{-1}. The base activity increased concomitantly with decreasing LDH crystallite size up to Si/(Mg + Al) atomic ratio of 0.17. However, above the Si/(Mg + Al) atomic ratio of 0.17, the reaction rate and TOF_{base} were decreased although the total base amount was increased. Results of TEM-EDS and ^{29}Si CP-MAS NMR suggest that the co-existing SiO_2 causes advantages for dispersion and reduction of the LDH crystallite to improve the base catalysis of SiO_2@Mg–Al LDH, whereas the excess SiO_2 species unfortunately poisons the highly active sites on the finely crystallized LDH crystals above a Si/(Mg + Al) atomic ratio of 0.17. According to these results, we inferred that the amount of spherical SiO_2 seeds in the co-precipitation method is an important factor to increase the base catalysis of SiO_2@LDHs; *i.e.* the control of Si/(Mg + Al) atomic ratio is necessary to avoid the poisoning of highly active base sites on the LDH crystal.

Introduction

Heterogeneous solid catalysts have been widely used in various chemical reactions in the chemical industry, exhaust gas purification, and environmentally friendly reactions. They are more suitable for reactions at high temperatures than homogeneous catalysts, and are removed easily from the reactor. In particular, solid acid catalysts are used in many important processes related to petroleum refining and petrochemical production. Consequently, numerous studies have specifically examined solid acid catalysts. On the other hand, fewer efforts have been devoted to heterogeneous base catalysts.[1] Because general base sites on a solid base catalyst are readily poisoned by moisture and carbon dioxide in the atmosphere,[2] the development of a promotion strategy for solid base catalysts is more difficult than for solid acid catalysts.

Layered double hydroxide, generally called LDH, is a well-known layered clay mineral that is known to act as a unique solid base catalyst. Actually, LDH comprises brucite-like positively charged two-dimensional sheets denoted as $[M_{1-x}^{2+}M_x^{3+}(OH)_2]^{x+}$ and interlayer parts denoted as $A_{x/n}^{n-} \cdot mH_2O$, where A^{n-} corresponds to interlayer anions such as carbonate and hydroxide. The positively charged sheets and the interlayers are alternately laminated to compensate for the charge between sheets.[3–5] Base sites on LDH are mainly regarded as identical Brønsted basic OH^- and HCO_3^- anions, which are adsorbed onto the LDH surface. These unique basic sites can act even in an air atmosphere and can exhibit basic characteristics without pretreatment.[4] As a solid base catalyst, LDH is well-known to catalyze various organic transformations such as aldol condensation,[6–9] Knoevenagel condensation,[10–13] epoxidation,[14–16] and transesterification.[17–19] Recent studies have indicated that LDHs can promote advanced environmentally friendly reactions such as biomass-derived saccharide conversion[13,20–25] and photocatalytic conversion of CO_2 in an aqueous solution.[26–28] Therefore, the development of highly active LDH catalysts is eagerly sought.

The main base sites on the LDH surface are generally regarded as adsorbed anions located at the corner and edge of a crystal.[29] However, the anions in the interlayer space cannot participate in the chemical reactions because of the high charge density of the LDH layers and the high contents of anionic species and water molecules, resulting in strong interlayer electrostatic interactions between the sheets.[4,30] Therefore, the delamination of LDH nanosheets[30–36] and the fine crystallization of LDH on appropriate carriers[37–42] have been conducted to increase the number of exposed active base sites. As-prepared LDH materials also have been evaluated carefully to assess their characteristics and utility as photocatalysts and electrocatalysts,[43,44] high active base catalysts for Knoevenagel condensation[45] and epoxidation,[46] magnetic separation of proteins,[37] pseudocapacitance,[38] flame retardancy of epoxy

[a]*School of Materials Science, Japan Advances Institute of Science and Technology, 1-1 Asahidai, Nomi, Ishikawa, 923-1292, Japan. E-mail: s_nishim@jaist.ac.jp; Fax: +81-761-51-1149; Tel: +81-761-51-1613*

[b]*Graduate School of Advanced Science and Technology, Japan Advances Institute of Science and Technology, Japan*

† Electronic supplementary information (ESI) available: Reactivity of SiO2@Mg–Al LDH. See DOI: 10.1039/c8ra04925d

resins,[40] and as adjuvants.[41] Nevertheless, no report describes a study of improvement of base catalysis of LDH itself by fine crystallization followed by *in situ* growth method of SiO_2@LDH nanoparticles.

An earlier study revealed a co-precipitation method for preparation of small-crystallized LDH catalysts on SiO_2 nanospheres and explored the superior base catalyses for the Knoevenagel condensation of benzaldehyde compared with conventional LDHs.[47] This method is applicable for the preparation of SiO_2@LDH nanoparticles with various compositions and element combinations: *i.e.* SiO_2@M^{2+}–M^{3+}LDH (M^{2+}: Mg^{2+} or Ni^{2+}, M^{3+}: Al^{3+} or Ga^{3+}, and M^{2+}/M^{3+}: 1 or 3). Various characterizations of SiO_2@LDH nanoparticles using XRD, TEM-EDS, and ^{29}Si CP-MAS NMR techniques revealed that the co-existence of small SiO_2 sphere (*ca.* 40 nm diameter) surface generated the starting points of LDH growth *via* Si–O–M covalent bond formation, leading to the formation of fine-crystallized LDH and enhancement of base catalysis for the Knoevenagel condensation of benzaldehyde with ethyl cyanoacetate. However, the roles of Si–O–M covalent bonds in the fine-crystallization of LDH and base catalysis have not been explored well. Therefore, in this paper, we investigated the base properties and structural parameters of as-prepared SiO_2@Mg–Al LDH materials with $Mg^{2+}/Al^{3+} = 3$, and discussed the base catalysis with different Si to (Mg + Al) ratios to reveal the mechanism of our strategy.

Experimental

Materials and synthesis of catalysts

Tetraethyl orthosilicate (TEOS), triethanolamine (TEA), and benzaldehyde were purchased from Sigma-Aldrich Corp. Sodium carbonate (Na_2CO_3), sodium hydroxide (NaOH) and toluene were supplied by Kanto Chemical Co. Inc. Cetyltrimethylammonium bromide (CTAB), magnesium nitrate hexahydrate ($Mg(NO_3)_2 \cdot 6H_2O$), aluminum nitrate enneahydrate ($Al(NO_3)_3 \cdot 9H_2O$), benzaldehyde and benzoic acid were obtained from Wako Pure Chemical Industries Ltd. Benzaldehyde was purified by distillation under 0.4 Pa pressure. Ethyl cyanoacetate was purchased from Tokyo Chemical Industry Co. Ltd. and was used without further purification.

Spherical SiO_2 (40 nm) was prepared according to descriptions in earlier reports.[41,46] First, 96 mmol of TEA and 2 mL of TEOS were combined in a 200 mL eggplant flask. The two-phase mixture was heated in an oil bath at 363 K for 20 min without stirring. When the mixture was removed from the oil bath, 26.0 mL of an aqueous solution (2.8 wt%) of CTAB pre-heated at 333 K was added immediately as a structure-directing agent in a condensation process. Then, it was stirred continuously for 24 h at room temperature. Thereafter, the resulting mixture was added to 50 mL of ethanol to obtain colloidal aqueous suspension. The obtained precipitate was centrifuged for 5 min at 4000 rpm. After decantation, the sediment was re-dispersed through vigorous stirring in 50 mL of an ethanolic solution of ammonium nitrate (20 g L^{-1}), and then refluxed for 1 h. This procedure was repeated three times. The same operation was performed with a solution of concentrated hydrochloric acid in ethanol (5 g L^{-1}) to replace the ammonium ions. The final sediment was washed with ethanol, and then dried *in vacuo*. The obtained spherical SiO_2 powder was calcined at 823 K under 1 L min^{-1} of air flow for 6 h.

The SiO_2@(Z)LDH catalysts (Z: desired Si/(Mg + Al) atomic ratio) were prepared *via* an *in situ* co-precipitation method according to a previous report.[42] Spherical SiO_2 (40 nm) was dispersed in 20 mL of water using ultrasound treatment. After 30 min, 0.96 mmol of Na_2CO_3 was added to the solution. Then, after an additional 5 min of sonication was conducted, 19.2 mL of metal nitrate aqueous solution ([Mg] + [Al] = 0.075 M) was slowly dropped into the spherical SiO_2 dispersed solution, followed by stirring at room temperature. The pH was maintained at 10.0 by an aqueous NaOH solution (1 M) during titration. The obtained suspension was stirred for an additional 1 h. After the resulting paste was filtered, it was washed with 1 L of water and ethanol. Then, it was dried at 383 K overnight. The Si/(Mg^{2+} + Al^{3+}) atomic ratios were varied from 0 to 0.50 whereas the Mg/Al atomic ratio was adjusted to 3.

Reaction

Knoevenagel condensation of benzaldehyde with ethyl cyanoacetate was proceeded in a 20 mL Schlenk tube under an N_2 flow (30 mL min^{-1}). The reaction was performed using 1.0 mmol of benzaldehyde, 1.2 mmol of ethyl cyanoacetate, 10 mg of catalysts and 3 mL of toluene at 313 K. The obtained products were analyzed using a GC-FID (GC-2014, Shimadzu Corp.) equipped with a polar column (DB-FFAP, Agilent Technologies Inc.).

Characterizations

X-ray diffraction patterns (XRD) were collected using a SmartLab (Rigaku Corp.) with a Cu Kα X-ray source (40 kV, 30 mA). The LDH (003) and (110) crystallite sizes were calculated using

Table 1 Chemical compositions of as-prepared SiO_2@(Z)LDHs estimated by ICP-AES

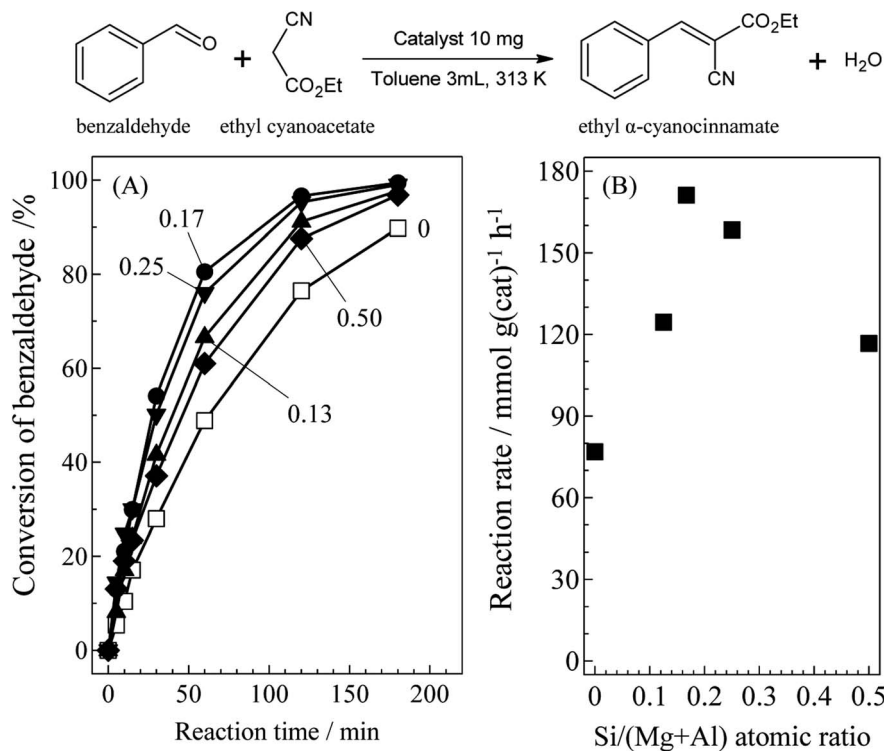| Sample	Si/(M^{2+} + M^{3+}) ratio		M^{2+}/M^{3+} ratio	
	Precursor	Obtained material	Precursor	Obtained material
LDH(CP)			3.0	2.8
SiO_2@(0.13)LDH	0.13	0.14	3.0	2.5
SiO_2@(0.17)LDH	0.17	0.18	3.0	2.6
SiO_2@(0.25)LDH	0.25	0.28	3.0	2.5
SiO_2@(0.50)LDH	0.50	0.53	3.0	2.2

Fig. 1 Activities for Knoevenagel condensation of benzaldehyde with ethyl cyanoacetate over as-prepared SiO$_2$@LDHs with various Si/(Mg + Al) atomic ratio; (A) time-based reaction progression on benzaldehyde conversion and (B) reaction rate. Reaction conditions: benzaldehyde (1.0 mmol), ethyl cyanoacetate (1.2 mmol), catalyst (10 mg), toluene (3 mL), 313 K, N$_2$ flow (30 mL min^{-1}). Number in (A) denotes Si/(Mg + Al) atomic ratio.

the Scherrer equation: $D_{hkl} = K\lambda/(\beta \cos \theta)$ (K: Scherrer number (0.9), λ: incident ray wavelength (0.1542 nm), β: peak width at half height (rad), θ; Bragg angle). ^{29}Si cross polarization magic angle spinning nuclear magnetic resonance (^{29}Si CP-MAS NMR) measurements were obtained by an Avance III 500 (Bruker Analytik GmbH) in a 4 mm ZrO$_2$ rotor. The spinning rate was 8 kHz. The ^{29}Si chemical shifts are referenced to hexamethylcyclotrisiloxane (taken to be at $\delta = -9.6875$ ppm). Transmission electron microscope – energy dispersive X-ray spectroscopy (TEM-EDS) elemental mapping analytical techniques were done with a JEM-ARM200F (JEOL) at 200 kV. Inductively coupled plasma – atomic emission spectrometry (ICP-AES) was operated by an iCAP 6300 Duo (Thermo Fisher Scientific Inc.) to estimate the actual amount of precipitated M(OH)$_x$ and SiO$_2$ in as-prepared SiO$_2$@Mg–Al LDHs with various Si/(Mg + Al) atomic ratio.

Results and discussion

Optimization of Si/(Mg + Al) ratio in SiO$_2$@LDH

We prepared SiO$_2$@LDHs with various loading amounts of SiO$_2$ to ascertain the optimized SiO$_2$@LDH structure for high catalytic reactivity. The sphere morphology and the diameter of SiO$_2$ were confirmed from SEM and TEM observations, as presented in an earlier report.[47] The correlation between Si/(Mg + Al) atomic ratio, base catalysis, and structural properties of SiO$_2$@LDHs were investigated in the range of 0–0.50 on Si/(Mg +
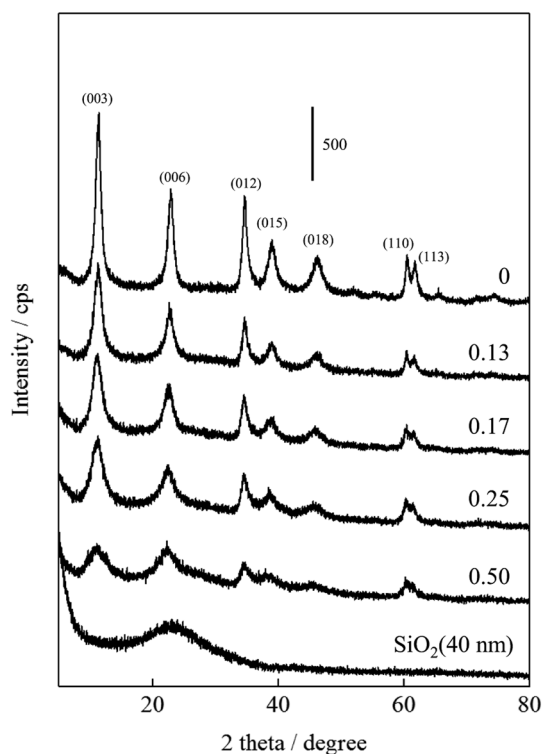

Fig. 2 XRD patterns of as-prepared SiO$_2$@LDHs with various Si/(Mg + Al) atomic ratio.

Table 2 Crystal properties of as-prepared SiO$_2$@LDHs with various Si/(Mg + Al) atomic ratio

Si/(Mg + Al) atomic ratio	Lattice parameter c/nm	Crystallite size (003)^a/nm	Lattice parameter a/nm	Crystallite size (110)^a/nm
0	2.33	7.6	0.31	13.4
0.13	2.32	5.2	0.31	13.7
0.17	2.36	4.5	0.31	10.3
0.25	2.38	3.7	0.31	8.0
0.50	2.43	2.8	0.31	8.3

^{a} The crystallite sizes of LDHs were calculated by Scherrer equation: $D_{hkl} = K\lambda/(\beta \cos \theta)$ (K: Scherrer number (0.9), λ: incident ray wavelength (0.1542 nm), β: peak width at half height (rad)).

Al) atomic ratio. The prepared catalysts are designated as SiO$_2$@(Z)LDH, where Z is a Si/(Mg + Al) atomic ratio. The actual ratios of Si/(M^{2+} + M^{3+}) and M^{2+}/M^{3+} in the obtained materials are presented in Table 1.

Fig. 1 presents catalytic activity for the Knoevenagel condensation over SiO$_2$@(Z)LDHs as (A) time-based reaction progression on benzaldehyde conversion and (B) reaction rate. The detailed results are listed in Table S1 (see ESI†). Among various Si/(Mg + Al) atomic ratio from 0 to 0.50, actually, the 0.17 was found to be the best catalyst with a reaction rate of 171.1 mmol g(cat)$^{-1}$ h^{-1}. This reaction rate is 2.2 times higher than conventional LDH prepared with the same co-precipitation method without SiO$_2$ seeds (Si/(Mg + Al) = 0).

The XRD patterns and crystal properties of SiO$_2$@(Z)LDHs are portrayed respectively in Fig. 2 and Table 2. All prepared catalysts showed an LDH-originated diffraction pattern. The intensity of LDH originated peaks decreased in accordance with Si loading amount, whereas that of amorphous SiO$_2$ increased slightly. Lattice parameters a and c, respectively calculated from LDH (003) and (110) diffraction peaks, are almost identical among Si/(Mg + Al) atomic ratios of 0–0.50. This result indicates clearly that these SiO$_2$@(Z)LDHs have the same LDH crystal unit. However, the crystallite size of LDH is unquestionably affected by Si/(Mg + Al) atomic ratio. The crystallite size of D(003) is reduced in accordance with the Si loading amount. The crystallite size of D(110) is almost identical in the region among Si/(Mg + Al) ratio of 0–0.13, but it is reduced from *ca.* 13 nm to 8 nm when a Si/(Mg + Al) ratio increased. In our earlier research, it was revealed that the co-precipitation method with co-existence of spherical SiO$_2$ caused dispersion of starting points of LDH crystal growth on the SiO$_2$ surface through the Si–O–Al and Si–O–Mg covalent bonds to lead generation of fine-crystallized LDH nanocrystal.[47] Fig. 3(A) shows that the spherical SiO$_2$ (40 nm) showed three peaks at −91, −100 and −109 ppm, which respectively correspond to Q^2, Q^3, and Q^4 species[48–50] where Q^n designated the Si-centered tetrahedral structural species; Q refers to silicon atom and n denotes the number of bridging oxygens. Furthermore, SiO$_2$@(Z)LDHs showed broad resonance between −70 to −115 ppm, which include some peaks attributed to Q^0 and/or Q^1 (−60 to −83 ppm)[49] and a Si-centered tetrahedral structure that possesses Si–O–Al and Si–O–Mg bonds (−73 to −105 ppm).[42]

These results suggest that, in the case of lower Si/(Mg + Al) atomic ratio (<0.13), the LDH crystal is immobilized onto the

SiO$_2$ surface through the Si–O–Al and Si–O–Mg bonds to inhibit *ab*-face stacking without reducing the plane crystallite size. This result seems to be attributable to the lower number of starting points of LDH crystal growth: the amount of metal constituting one crystal did not change compared with conventional LDH prepared without SiO$_2$ seeds (Si/(Mg + Al) = 0). Actually, the proportion for the ^{29}Si CP-MAS NMR peaks attributed to Si–O–Mg and Si–O–Al bonds on the SiO$_2$@(0.13)LDH is only ≤40%, whereas that of SiO$_2$@(0.17)LDH is ≤61%, as shown in Fig. 3 and Table 3. Therefore, we infer that the number of Si–O–Mg and Si–O–Al bonds on the SiO$_2$ surface deeply affected
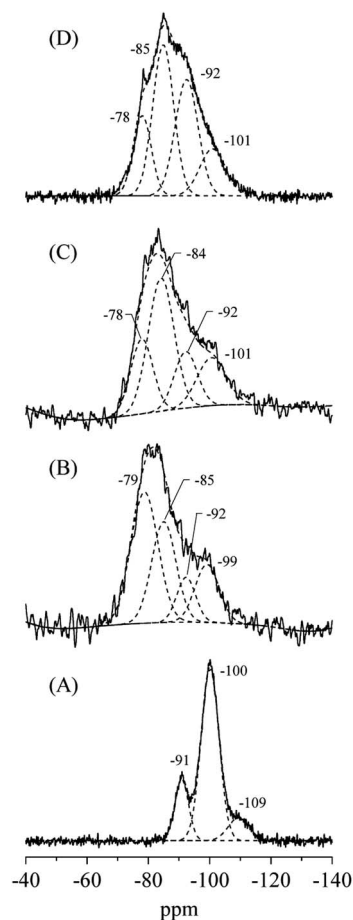

Fig. 3 ^{29}Si CP-MAS NMR spectra of (A) spherical SiO$_2$ (40 nm), (B) SiO$_2$@(0.13)LDH, (C) SiO$_2$@(0.17)LDH and (D) SiO$_2$@(0.50)LHD.

Table 3 Surface area and silicon environments in the SiO_2 and SiO_2@(Z)LDHs as determined by ^{29}Si CP-MAS NMR

Sample	Assignment	δ/ppm	Percentage/%
SiO_2 (40 nm)	Q^4	−109	11
sphere	Q^3	−100	70
	Q^2	−91	19
SiO_2@(0.13)LDH	Q^3	−99	17
	Q^2	−92	10
	Q^4(3Al), Q^3(1Mg)		
	Q^4(4Al), Q^3(1Al), Q^2(1Mg)	−85	30
	Q^1 and/or Q^0	−79	43
SiO_2@(0.17)LDH	Q^3	−100	18
	Q^2	−92	17
	Q^4(3Al), Q^3(1Mg)		
	Q^4(4Al), Q^3(1Al), Q^2(1Mg)	−85	44
	Q^1 and/or Q^0	−78	21
SiO_2@(0.50)LDH	Q^3	−101	14
	Q^2	−92	31
	Q^4(3Al), Q^3(1Mg)		
	Q^4(4Al), Q^3(1Al), Q^2(1Mg)	−85	37
	Q^1 and/or Q^0	−78	17

reduction of the crystallite size not only in the stacking direction but also in the plane direction when below Si/(Mg + Al) < 0.17–0.25.

Correlation between the base amount and catalytic activity for Knoevenagel condensation over SiO_2@(Z)LDHs is presented in Table 4. Although the base amount of SiO_2@(0.13)LDH was lower than that of conventional LDH, the reaction rate and the apparent TOF per base site (TOF_{base}) for SiO_2@(0.13)LDH are higher than those of LDH. The D(003) of SiO_2@(0.13)LDH was smaller than LDH, whereas D(110) of SiO_2@(0.13)LDH and LDH are almost identical, as shown in Table 2. Therefore, these indicated that the immobilization of LDH crystal onto SiO_2 with inhibition of the *ab*-face stacking led to increase in the number of highly active base sites located on the surface LDH layer. Above the Si/(Mg + Al) atomic ratio of 0.13, a base amount increased in accordance with Si/(Mg + Al) ratio from 0.32 to 0.49 mmol g(cat)$^{-1}$. Furthermore, the activity was maximized at

Si/(Mg + Al) ratio of 0.17 with the reaction rate of 171.1 mmol g(cat)$^{-1}$ h^{-1}. It is particularly interesting that the reaction rate per obtained LDH phase and TOF_{base} were also maximized at Si/(Mg + Al) ratio of 0.17 with the reaction rate of 193.6 mmol g(LDH)$^{-1}$ h^{-1} and TOF_{base} of 450 h^{-1}. Above the Si/(Mg + Al) ratio of 0.17, both the reaction rate per LDH phase and TOF_{base} were decreased respectively to 158.4 mmol g(LDH)$^{-1}$ h^{-1} and 238 h^{-1} at Si/(Mg + Al) ratio of 0.50. These results strongly suggest that the Si/(Mg + Al) atomic ratio affects not only the LDH crystallite size and base amount but also the type of base sites and these fractions.[51]

The LDH crystallite size of SiO_2@(0.50)LDH is at least smaller than that of SiO_2@(0.17)LDH. Therefore, the base catalysis of SiO_2@(0.50)LDH is expected to be better than that of SiO_2@(0.17)LDH if the base catalysis is only influenced by the crystallite size. ^{29}Si CP-MAS NMR spectra showed that the proportion of terminal Si–OH species assigned as Q^0 and/or Q^1 decreased in accordance with Si/(Mg + Al) atomic ratio, as shown in Table 3, indicating first that a surface Si–O–Si bond is cleaved to generate terminal Si–OH species and then that these act as cross-link point with Mg and Al ions. Consequently, when there are the excess free terminal Si–OH species in the solution after the generation of SiO_2@LDH, these excess Si–OH species cover the LDH crystal to produce Si–O–Mg and Si–O–Al covalent bonds. Although the base amount is increased even the region from SiO_2@(0.13)LDH to SiO_2@(0.50)LDH, this phenomenon might take place only with difficulty on the inferior base sites located at a flat plane of LDH. However, the decrease of TOF_{base} strongly suggests that the high active base sites are poisoned by Si species in the case of a higher Si/(Mg + Al) atomic ratio.

Dark-field TEM images and results of EDS elemental mapping of SiO_2@(Z)LDHs are presented in Fig. 4. In the case of lower Si/(Mg + Al) atomic ratio such as 0.13 and 0.17, the LDH crystal is generated with covering the SiO_2 phase to form a SiO_2 core – LDH shell-like structure, as shown in Fig. 4(A)–(J). Furthermore, results show that the boundary between SiO_2 phase and LDH phase becomes ambiguous in accordance with the increase of Si/(Mg + Al) atomic ratio (Fig. 4(K)–(T)). These indicate that first the LDH crystal grows up from the SiO_2 surface to generate the immobilized SiO_2 core – LDH shell structure. If there are excess dissolved SiO_2 species possessing

Table 4 Activity for the Knoevenagel condensation and base amount of as-prepared SiO_2@(Z)LDHs

Sample	Amount of LDH^a/wt%	Reaction rate^b		Base amount^c /mmol g(cat)$^{-1}$	TOF_{base}/h^{-1}
		mmol g(cat)$^{-1}$ h^{-1}	mmol g(LDH)$^{-1}$ h^{-1}		
LDH(CP)	100	76.9	76.9	0.42	183
SiO_2@(0.13)LDH	90.8	124.5	137.0	0.32	389
SiO_2@(0.17)LDH	88.3	171.1	193.6	0.38	450
SiO_2@(0.25)LDH	82.9	158.4	191.0	0.40	396
SiO_2@(0.50)LDH	73.6	116.7	158.4	0.49	238

^{a} The amount of LDH in the SiO_2@(Z)LDHs was calculated by ICP-AES with an assumption: all SiO_2@(Z)LDHs are composed of mixture of LDH and SiO_2. ^{b} Reaction rate for the Knoevenagel condensation of benzaldehyde with ethyl cyanoacetate. ^{c} Base amount calculated from poisoning test by benzoic acid titration.
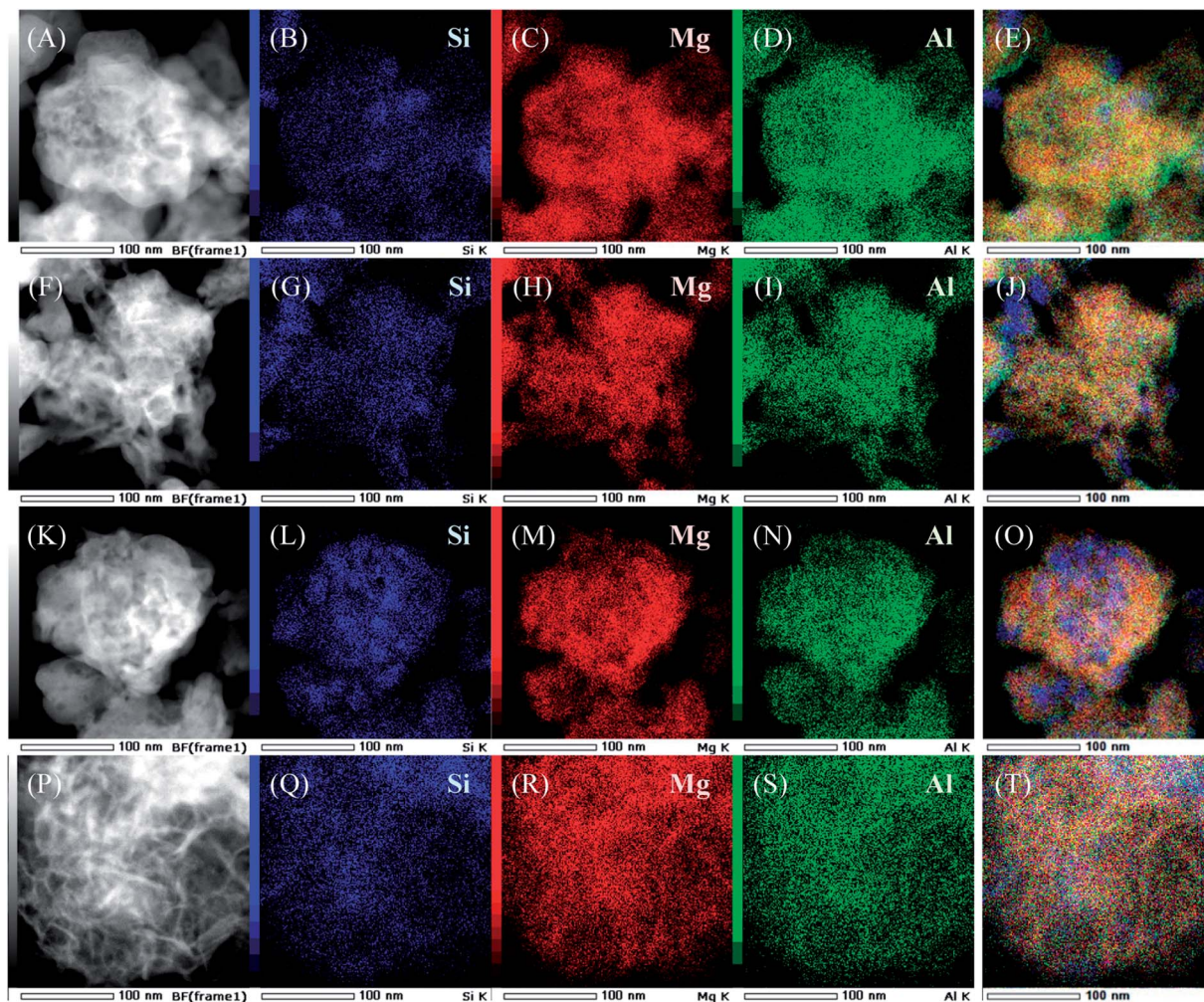
Fig. 4 (A, F, K and P) Dark-field TEM images of as-prepared SiO$_2$@LDHs with various Si/(Mg + Al) atomic ratio: (A) 0.13, (F) 0.17, (K) 0.25 and (P) 0.50. Also shown are (B–E), (G–J), (L–O), (Q–T) EDS mapping results of as-prepared SiO$_2$@LDH with various Si/(Mg + Al) atomic ratio.

a free terminal Si–OH group, then these produced Si–O–Mg and Si–O–Al covalent bonds with the LDH crystal to cover the LDH shell.

Accordingly, we infer the correlation between Si/(Mg + Al) atomic ratio and base catalysis of prepared SiO$_2$@(Z)LDHs as follows: (i) below Si/(Mg + Al) atomic ratio of 0.13, the LDH crystal is just immobilized onto the SiO$_2$ surface with inhibition of the *ab*-face stacking. The exposed corner and edge located at the surface layer act as highly active base sites. (ii) Fine crystallization occurs not only in the stacking direction, but also in the plane direction to increase the amount of base sites, especially base sites with high activity up to Si/(Mg + Al) atomic ratio of 0.17. (iii) Above a Si/(Mg + Al) atomic ratio of 0.17, excess terminal Si–OH species covered the highly active base sites to produce Si–O–Mg and Si–O–Al covalent bonds, thereby lowering the activity.

Conclusions

The effects of SiO$_2$ loading amounts on the crystallite sizes, basicity, and catalytic activity of SiO$_2$@LDH catalysts were

investigated. SiO$_2$@LDHs were prepared using co-precipitation with the coexistence of various amounts of spherical SiO$_2$ with particle sizes of *ca.* 40 nm. The XRD results suggest that the LDH crystallite size of D(003) is simply reduced in accordance with the Si loading amount. Furthermore, the crystallite size of D(110) is almost identical below Si/(Mg + Al) of 0.13, although it is reduced above 0.13. Base catalysis of SiO$_2$@LDHs was evaluated using Knoevenagel condensation of benzaldehyde and ethyl cyanoacetate. Both the reaction rate and the apparent TOF per base site were increased in the region between Si/(Mg + Al) atomic ratio of 0–0.17, whereas the base amount is increased linearly from the Si/(Mg + Al) atomic ratio of 0.13 to 0.50 with reduction of the LDH crystallite size. The results of ^{29}Si CP-MAS NMR and STEM-EDS suggest that a surface Si–O–Si bond is cleaved, generating terminal Si–OH species that act as a cross-link point with Mg and Al ions to form an immobilized SiO$_2$ core – LDH shell structure. However, when the amount of Si becomes excessive with respect to Mg and Al ions, the excess Si–OH group forms Si–O–Mg and Si–O–Al covalent bonds with LDH crystal to cover the LDH shell. From these results, we inferred the effect of SiO$_2$ amount on heterogeneous base

catalysis of SiO$_2$@Mg–Al LDH as follows: (i) below Si/(Mg + Al) atomic ratio of 0.13, the highly active base sites located at the corner and edge of surface layer are exposed by immobilization of LDH crystals onto the SiO$_2$ surface, (ii) up to Si/(Mg + Al) atomic ratio of 0.17, the number of exposed highly active base sites is increased in accordance with reduction of LDH crystallite, and (iii) above Si/(Mg + Al) atomic ratio of 0.17. Excess terminal Si–OH species covered the highly active base sites through the Si–O–Mg and Si–O–Al covalent bonds to decrease the activity. This study elucidated the correlation between SiO$_2$ amount, crystal properties, and the basicity of fine-crystallized SiO$_2$@LDH catalysts to present a new technique to improve the base catalysis of the widely used LDH material. After optimization of the Si/(Mg + Al) atomic ratio in SiO$_2$@LDHs, the Si/(Mg + Al) atomic ratio of 0.17 was found to be the best catalyst, with the reaction rate of 171.1 mmol g(cat)$^{-1}$ h^{-1}, which is a 2.2 times higher value than that of the conventional LDH prepared with same protocol in absence of SiO$_2$ seed agents.

Conflicts of interest

There are no conflicts to declare.

Acknowledgements

References

1 Y. Ono and H. Hattori, *Solid Base Catalysis*, Tokyo Institute of Technology Press, Tokyo, Japan, 2011.

2 H. Hattori, *Appl. Catal., A*, 2001, **222**, 247–259.

3 S. Miyata, *Clays Clay Miner.*, 1980, **28**, 50–56.

4 S. Nishimura, A. Takagaki and K. Ebitani, *Green Chem.*, 2013, **15**, 2026–2042.

5 P. J. Sideris, U. G. Nielsen, Z. Gan and C. P. Grey, *Science*, 2008, **321**, 113–117.

6 Z. An, W. Zhang, H. Shi and J. He, *J. Catal.*, 2006, **241**, 319–327.

7 H. C. Greenwell, P. J. Holliman, W. Jones and B. V. Velasco, *Catal. Today*, 2006, **114**, 397–402.

8 L. Hora, V. Kelbichová, O. Kikhtyanin, O. Bortnovskiy and D. Kubička, *Catal. Today*, 2014, **223**, 138–147.

9 D. G. Crivoi, R. A. Miranda, E. Finocchio, J. Llorca, G. Ramis, J. E. Sueiras, A. M. Segarra and F. Medina, *Appl. Catal., A*, 2016, **519**, 116–129.

10 M. L. Kantam, B. M. Choudary, C. V. Reddy, K. K. Rao, M. L. Kantam, B. M. Choudary, K. K. Rao and F. Figueras, *Chem. Commun.*, 1998, 1033–1034.

11 M. J. Climent, S. Iborra, K. Epping and A. Velty, *J. Catal.*, 2004, **225**, 316–326.

12 E. Angelescu, O. D. Pavel, R. Bîrjega, R. Zăvoianu, G. Costentin and M. Che, *Appl. Catal., A*, 2006, **308**, 13–18.

13 M. Shirotori, S. Nishimura and K. Ebitani, *Catal. Sci. Technol.*, 2014, **4**, 971–978.

14 K. Yamaguchi, K. Mori, T. Mizugaki, K. Ebitani and K. Kaneda, *J. Org. Chem.*, 2000, **65**, 6897–6903.

15 T. Honma, M. Nakajo, T. Mizugaki, K. Ebitani and K. Kaneda, *Tetrahedron Lett.*, 2002, **43**, 6229–6232.

16 O. D. Pavel, B. Cojocaru, E. Angelescu and V. I. Pârvulescu, *Appl. Catal., A*, 2011, **403**, 83–90.

17 M. Fuming, P. Zhi and L. Guangxing, *Org. Process Res. Dev.*, 2004, **8**, 372–375.

18 E. Li, Z. P. Xu and V. Rudolph, *Appl. Catal., B*, 2009, **88**, 42–49.

19 J. Nowicki, J. Lach, M. Organek and E. Sabura, *Appl. Catal., A*, 2016, **524**, 17–24.

20 M. Ohara, A. Takagaki, S. Nishimura and K. Ebitani, *Appl. Catal., A*, 2010, **383**, 149–155.

21 A. Takagaki, M. Ohara, S. Nishimura and K. Ebitani, *Chem. Lett.*, 2010, **39**, 838–840.

22 A. Takagaki, M. Takahashi, S. Nishimura and K. Ebitani, *ACS Catal.*, 2011, **1**, 1562–1565.

23 J. Tuteja, S. Nishimura and K. Ebitani, *Bull. Chem. Soc. Jpn.*, 2012, **85**, 275–281.

24 M. Shirotori, S. Nishimura and K. Ebitani, *Chem. Lett.*, 2016, **45**, 194–196.

25 M. Shirotori, S. Nishimura and K. Ebitani, *Catal. Sci. Technol.*, 2016, **6**, 8200–8211.

26 K. Teramura, S. Iguchi, Y. Mizuno, T. Shishido and T. Tanaka, *Angew. Chem., Int. Ed.*, 2012, **51**, 8008–8011.

27 S. Iguchi, K. Teramura, S. Hosokawa and T. Tanaka, *Catal. Today*, 2015, **251**, 140–144.

28 S. Iguchi, K. Teramura, S. Hosokawa and T. Tanaka, *Phys. Chem. Chem. Phys.*, 2016, **18**, 13811–13819.

29 M. B. Roeffaers, B. F. Sels, I. H. Uji, F. C. de Schryver, P. A. Jacobs, D. E. de Vos and J. Hofkens, *Nature*, 2006, **439**, 572–575.

30 M. Adachi-Pagano, C. Forano and J. P. Besse, *Chem. Commun.*, 2000, 91–92.

31 E. Gardner, K. M. Huntoon and T. J. Pinnavaia, *Adv. Mater.*, 2001, **13**, 1263–1266.

32 S. O'Leary, D. O'Hare and G. Seeley, *Chem. Commun.*, 2002, 1506–1507.

33 T. Hibino, *Chem. Mater.*, 2004, **16**, 5482–5488.

34 W. Chen, L. Feng and B. Qu, *Chem. Mater.*, 2004, **16**, 368–370.

35 Z. Liu, R. Ma, M. Osada, N. Iyi, Y. Ebina, K. Takada and T. Sasaki, *J. Am. Chem. Soc.*, 2006, **128**, 4872–4880.

36 H. Kang, Y. Shu, Z. Li, B. Guan, S. Peng, Y. Huang and R. Liu, *Carbohydr. Polym.*, 2014, **100**, 158–165.

37 M. Shao, F. Ning, J. Zhao, M. Wei, D. G. Evans and X. Duan, *J. Am. Chem. Soc.*, 2012, **134**, 1071–1077.

38 M. Shao, F. Ning, Y. Zhao, J. Zhao, M. Wei, D. G. Evans and X. Duan, *Chem. Mater.*, 2012, **24**, 1192–1197.

39 C. Chen, P. Wang, T. T. Lim, L. Liu, S. Liu and R. Xu, *J. Mater. Chem. A*, 2013, **1**, 3877–3880.

40 S. D. Jiang, Z. M. Bai, G. Tang, L. Song, A. A. Stec, T. R. Hull, Y. Hu and W. Z. Hu, *ACS Appl. Mater. Interfaces*, 2014, **6**, 14076–14086.

41 J. Wang, R. Zhu, B. Gao, B. Wu, K. Li, X. Sun, H. Liu and S. Wang, *Biomaterials*, 2014, **35**, 466–478.

42 C. Chen, R. Felton, J. C. Buffet and D. O'Hare, *Chem. Commun.*, 2015, **51**, 3462–3465.

43 J. L. Gunjakar, T. W. Kim, H. N. Kim, I. Y. Kim and S. J. Hwang, *J. Am. Chem. Soc.*, 2011, **133**, 14998–15007.

44 C. Zhang, J. Zhao, L. Zhou, Z. Li, M. Shao and M. Wei, *J. Mater. Chem. A*, 2016, **4**, 11516–11523.

45 T. Hara, J. Kurihara, N. Ichikuni and S. Shimazu, *Chem. Lett.*, 2010, **39**, 304–305.

46 J. Kobler, K. Möller and T. Bein, *ACS Nano*, 2008, **2**, 791–799.

47 M. Shirotori, S. Nishimura and K. Ebitani, *J. Mater. Chem. A*, 2017, **5**, 6947–6957.

48 N. Gunawidjaja, M. A. Holland, G. Mountjoy, D. M. Pickup, R. J. Newport and M. E. Smith, *Solid State Nucl. Magn. Reson.*, 2003, **23**, 88–106.

49 A. M. B. Silva, C. M. Queiroz, S. Agathopoulos, R. N. Correia, M. H. V. Fernandes and J. M. Oliveira, *J. Mol. Struct.*, 2011, **986**, 16–21.

50 M. Lewandowski, G. S. Babu, M. Vezzoli, M. D. Jones, R. E. Owen, D. Mattia, P. Plucinski, E. Mikolajska, A. Ochenduszko and D. C. Apperley, *Catal. Commun.*, 2014, **49**, 25–28.

51 Discussion on the surface area values of LDHs itself in as-prepared SiO_2@(Z)LDHs were hardly estimated because the obtained surface area in experiment included not only LDH shell but also SiO_2 core contributions. Note that a tentative discussion had been attempted in our previous paper of ref. 47.